

## Article

# Formulation by Design of an Innovative Tea Tree Oil Nanoemulgel Incorporating Mupirocin for Enhanced Wound Healing Activity

Mahdi M. Bujubarah <sup>1</sup>, Heba S. Elsewedy <sup>1,2,\*</sup>, Tamer M. Shehata <sup>1,3,\*</sup>  and Wafaa E. Soliman <sup>4,5</sup> 

<sup>1</sup> Department of Pharmaceutical Sciences, College of Clinical Pharmacy, King Faisal University, Alhofuf 36362, Saudi Arabia

<sup>2</sup> Department of Pharmaceutical Sciences, College of Pharmacy, Almaarefa University, Dariyah, Riyadh 13713, Saudi Arabia

<sup>3</sup> Department of Pharmaceutics, College of Pharmacy, Zagazig University, Zagazig 44519, Egypt

<sup>4</sup> Department of Biomedical Sciences, College of Clinical Pharmacy, King Faisal University, Alhofuf 36362, Saudi Arabia; weahmed@kfu.edu.sa

<sup>5</sup> Department of Microbiology and Immunology, Faculty of Pharmacy, Delta University for Science and Technology, Gamasa 11152, Egypt

\* Correspondence: hsewedy@um.edu.sa (H.S.E.); tshehata@kfu.edu.sa (T.M.S.)

**Abstract:** Mupirocin is an antibacterial agent that has been documented to be effective in treating superficial skin infections. However, the main limitation of its application is bacterial resistance. Therefore, there is a need to determine a way to potentiate its efficiency. Accordingly, this obstacle led to this current investigation, which aims to find a way to improve the therapeutic action of mupirocin. This study focuses on the integration of tea tree oil with mupirocin to improve its antibacterial and wound healing capacities. Distinct nanoemulsions (NEs) were developed and the best of them were optimized using a central composite design (CCD) approach. The optimized NEs were mixed with a gel base to form a mupirocin-loaded nanoemulgel (NEG). The formulation was evaluated for characteristics including pH, viscosity, spreadability, and in vitro release over 6 h. The NEG was examined for its stability in two different conditions, namely at room temperature and refrigerated, for 3 months. Eventually, the NEG was inspected to determine its antibacterial and wound healing efficiencies. The developed mupirocin-loaded NEG exhibited good physical properties in terms of pH (6.13), viscosity (19,990 cP), spreadability (48.8 mm), and in vitro release over 6 h (51.4%). Moreover, it showed good stability with no significant difference in the evaluated parameters when stored for 3 months in the two conditions. Ultimately, mupirocin-loaded NEG prepared with tea tree oil exhibited a significant antibacterial influence in addition to good healing efficiency.

**Keywords:** mupirocin; nanoemulgel; antibacterial; wound healing; natural product; tea tree oil



**Citation:** Bujubarah, M.M.; Elsewedy, H.S.; Shehata, T.M.; Soliman, W.E. Formulation by Design of an Innovative Tea Tree Oil Nanoemulgel Incorporating Mupirocin for Enhanced Wound Healing Activity. *Appl. Sci.* **2023**, *13*, 13244. <https://doi.org/10.3390/app132413244>

Academic Editor: Van-An Duong

Received: 17 October 2023

Revised: 29 November 2023

Accepted: 1 December 2023

Published: 14 December 2023



**Copyright:** © 2023 by the authors. Licensee MDPI, Basel, Switzerland. This article is an open access article distributed under the terms and conditions of the Creative Commons Attribution (CC BY) license (<https://creativecommons.org/licenses/by/4.0/>).

## 1. Introduction

Mupirocin is a secondary metabolite used as a topical antibiotic and works by attaching to certain bacterial enzymes, inhibiting them from synthesizing proteins [1]. Mupirocin is used for treating infections brought on by pathogens such as methicillin-resistant *Staphylococcus aureus* (MRSA) [2]. It has been shown that the antibacterial activity of mupirocin has a key role in the treatment of infected wounds. Nevertheless, there is growing proof that staphylococci are resistant to mupirocin as a result of its unrestricted use for treatment [3]. It was reported that using mupirocin in combination with other therapies provided more prominent and significant action in antibacterial influence and wound healing than mupirocin alone [4]. Therefore, in order to attain a more efficacious influence of mupirocin, it is better that it be used in combination with other treatments, such as natural products that have also shown certain antibacterial and wound healing activities.

Presently, natural products are broadly utilized as complementary medicines owing to their magnitude of influence in managing various disorders with higher safety and fewer side effects [5]. Essential oils are categorized as natural products and possess a variety of active components that possess strong influence in various aspects [6]. Tea tree oil is one such essential oil product, which is primarily obtained from the native Australian *Melaleuca alternifolia* tree [7]. Recently, many topical preparations containing tea tree oil as the active component have been used for treating cutaneous infections. Tea tree oil is greatly renowned for its documented antimicrobial activity owing to its monoterpenoid components [8]. According to previous studies regarding the antimicrobial effects of monoterpenes, it was stated that these compounds migrate into cell membranes and harm their structures [9]. Terpinen-4-ol is primarily responsible for the broad-spectrum antibacterial activity that is demonstrated by tea tree oil [10]. Regarding its wound healing efficiency, it has been described as a “magic” healing oil since it provides the most effective protection against infections caused by cuts, bites, and other wounds [10]. Consequently, incorporating tea tree oil in formulations containing antibacterial agents such as mupirocin would provide an extensive enhancement in wound healing behavior.

Emulsion is the best pharmaceutical preparation that contains oil as one of its main components. In line with recent approaches, nanotechnology is employed to obtain nanomedicine in a nanosized range, such as nanoemulsions (NEs). NEs are homogeneous dispersions formed of both aqueous and oily phases dispersed together using an emulsifying agent [11]. The advantages of NEs are their stability, small droplets, and enhanced physicochemical properties [12]. NEs can be used as carriers for numerous drugs to provide anticancer, antioxidant, anti-inflammatory, analgesic, antifungal, and antibacterial effects with wound healing activity [13–15]. Moreover, NEs can be used to deliver medication in various ways to achieve their pharmacological objectives, including parenteral, oral, transdermal, and topical routes [16–18].

Topical drug delivery is a method of treating skin disorders in an efficient and direct way that ensures good therapeutic impact due to the localization of the medication on the affected area [19]. A variety of conventional dosage forms can be used for topical application, namely cream, gel, paste, and ointment. However, certain challenges and limitations can be faced as a result of their bioavailability [20]. Such problems have forced the manufacturing of innovative topical drug delivery systems based on nanotechnology. Though NE is one of these innovative nanocarriers that can be utilized for delivering medication topically, its lower viscosity could lower its ability to stick to the affected area. Applying a formulation with higher viscosity is more efficient because it can be easily applied and spread over the skin and cannot be easily removed [21]. Therefore, an innovative nanoemulgel (NEG) was synthesized using NE after being mixed with preformulated gel.

NEG is widely used as a tool for topical drug delivery because it can incorporate both lipophilic and hydrophilic drugs. Additionally, it enhances the stability of the formulation through reductions in surface and interfacial tension, which raises its viscosity, eases its application, and avoids gastrointestinal problems [22]. Additionally, several investigations emphasized that NEG provides more stability in formulations than NE, which raises aqueous phase viscosity through a reduction in surface and interfacial tensions [23]. Remarkably, in order to develop pharmaceutical products of the highest quality and with better attributes, it has been discovered that formulation by design (FbD) is a useful technique. This technique helps in the development of more effective, economical, and safe drug delivery systems towards the achievement of quality-by-design goals [24]. This requires a reasonable approach to experimental strategies, such as using a central composite design (CCD) approach.

In these contexts, the present study was an attempt to potentiate the influence of mupirocin as an antibacterial and wound healing agent. Employing a nanotechnology approach, NEs were developed, optimized, and incorporated into a gel base to attain an NEG formulation for better topical application. The NEG formulation was subjected to

various physical characterizations and evaluated to determine its antibacterial and wound healing efficiencies.

## 2. Materials and Methods

### 2.1. Materials

Mupirocin was obtained as a gift sample from AVALON PHARMA (Middle East Pharmaceutical Industries Co. Ltd., Riyadh, Saudi Arabia). Tea tree oil was purchased from NOW® Essential Oils (NOW Foods, Bloomingdale, IL, USA). Tween 80 was obtained from ALPHA CHEMIKA (Mumbai, India). Polyethylene glycol 400 was purchased from Merck KGaA® (Darmstadt, Germany). The gelling agent consisting of Na alginate was purchased from Sigma-Aldrich Co. (St. Louis, MO, USA). All other chemicals and solvents were of analytical grade.

### 2.2. Designing the Experiment

As a tool of Response Surface Methodology (RSM), a central composite design (CCD) approach was used to explore how some independent factors affected certain dependent responses in order to facilitate the supposition of the data. A strategy was developed in which three variables were examined to determine their impact on two responses, as shown in Table 1. The chosen independent variables were oil concentration (A), Tween 80 concentration (B), and PEG 400 concentration (C), along with their effect on two responses, namely particle size Y1 and in vitro release Y2. The Design-Expert version 12.0 software (Stat-Ease, Minneapolis, Minnesota, USA) was used to perform the study and demonstrate some data analysis using analysis of variance (ANOVA) tests. Additionally, the software generated modeling graphs that were supported by specific mathematical equations [25].

**Table 1.** Experimental runs for various mupirocin NEs produced via CCD and their observed dependent variables.

Formula	Independent Variables			Dependent Variables		
	A (%)	B (%)	C (%)	Particle Size (nm)	In Vitro Release (%)	PDI
F1	2.5	1	1.5	265 ± 3.2	50 ± 3.0	0.467 ± 0.061
F2	1.5	1	0.5	123 ± 2.0	75 ± 1.8	0.348 ± 0.034
F3	1.5	0.5	1.5	136 ± 2.5	73 ± 2.8	0.350 ± 0.049
F4	2	0.32	1	254 ± 3.4	53 ± 2.6	0.573 ± 0.048
F5	2	0.75	0.15	225 ± 1.9	55 ± 2.2	0.276 ± 0.013
F6	2	0.75	1	214 ± 3.0	59 ± 2.3	0.341 ± 0.032
F7	2	1.17	1	176 ± 2.9	65 ± 3.2	0.333 ± 0.031
F8	2.5	0.5	0.5	356 ± 4.5	42 ± 3.0	0.521 ± 0.024
F9	1.5	0.5	0.5	149 ± 2.5	69 ± 2.7	0.319 ± 0.019
F10	1.15	0.75	1	97 ± 2.0	81 ± 2.6	0.323 ± 0.035
F11	2	0.75	1	212 ± 3.2	60 ± 2.8	0.275 ± 0.010
F12	2	0.75	1.8	192 ± 1.7	62 ± 2.5	0.226 ± 0.007
F13	2.5	1	0.5	286 ± 3.6	47 ± 2.4	0.439 ± 0.018
F14	2	0.75	1	217 ± 3.5	57 ± 3.5	0.326 ± 0.012
F15	1.5	1	1.5	117 ± 2.1	79 ± 3.1	0.307 ± 0.021
F16	2.5	0.5	1.5	315 ± 4.7	45 ± 3.0	0.489 ± 0.018
F17	2.8	0.75	1	375 ± 3.4	40 ± 2.0	0.495 ± 0.010

A: Oil concentration; B: Tween 80 concentration; C: PEG 400 concentration; Y1 particle size; and Y2: in vitro release.

### 2.3. The Formulation of Nanoemulsions

Different NEs containing mupirocin were prepared and their compositions are displayed in Table 1. Different concentrations of TTO, Tween 80, and PEG 400 were mixed to form the oily phase in which mupirocin was dissolved. The oily phase was put in a water bath with continuous stirring using a vortex (classic vortex mixer, VELP Scientifica, Italy)

until well mixed. Further, water was added gradually to the oily phase. Both phases were heated to 70–80 °C and then homogenized using an Ultra-Turrax homogenizer (IKA-T25; Germany) for 5 min at 10,000 rpm to obtain a suitable particle size [26].

#### 2.4. The Characterization of Mupirocin-Loaded NE Formulations

##### 2.4.1. Particle Characterization

To determine the particle size distribution, a zetasizer instrument (Malvern Instruments Ltd., Worcestershire, UK) was utilized. This was determined by measuring their dynamic light scattering at 25 °C with a scattering angle of 90°. In brief, 3 mL of distilled water was used to dilute 10 microliters of mupirocin formulation; then, the particle size and polydispersity index of the NE preparations were measured [27].

##### 2.4.2. In Vitro Drug Release Study

By means of Franz diffusion cells (Logan Instruments Corp., FDC-6, Somerset, NJ, USA), the in vitro release of mupirocin from the formulated NEs was conducted. The donor and receptor chambers of the diffusion cell were separated by the cellulose acetate cellophane membrane (MWCO 2000–15,000), which was clamped, and freshly made phosphate buffer pH 5.5 was poured into the receptor chamber. The samples were taken out at predetermined intervals (0.25, 0.5, 1, 2, 3, 4, 5, and 6 h) and replaced with equivalent volumes of fresh buffer solution to maintain the volume constant throughout the testing period. After the proper dilutions, the samples were examined for drug content using a UV visible spectrophotometer (JENWAY 6305, Bibby Scientific Ltd., Staffs, UK) at  $\lambda_{\max}$  222 nm [28].

#### 2.5. The Formulation of Nanoemulgel

The optimized mupirocin-loaded NE formulation was inserted into a gel preparation in order to attain an NE formulation that could be applied easily over the affected area. Therefore, Na alginate gel (2%) was prepared where the gelling agent was added to 10 mL of distilled water and stirred continuously using a magnetic stirrer (Jeio Tech TM-14SB, Medline Scientific, Oxfordshire, UK) until a homogenous gel was produced. After that, the formed gel was mixed with NE formulations for 5 min using a mixer (Heidolph RZR1, Heidolph Instruments, Schwabach, Germany), resulting in a mupirocin-loaded NEG formulation.

#### 2.6. The Characterization of NE Formulation

##### 2.6.1. Visual Inspection

Following 48 h of preparation, the developed formulation was inspected for any physical changes including color and homogeneity [29].

##### 2.6.2. pH Determination

The pH of the formulation was measured using a pH meter (MW802, Milwaukee Instruments, Szeged, Hungary). The measurement was carried out by immersing the pH sensor probe in a dispersion formed from 0.5 g of formulation in 20 mL of distilled water. The measurement was carried out at ambient temperature [30].

##### 2.6.3. Viscosity Measurement

The viscosity of the mupirocin-loaded NEG formulation was evaluated using a Brookfield viscometer (DV-II+ Pro, USA). Simply, spindle No. 63 was utilized and rotated at a speed of 0.5 rpm to measure the viscosity. The measurements were carried out while a sample of the NEG was maintained at room temperature (25 °C) [31].

##### 2.6.4. Spreadability Test

This assessment is highly important for topical formulations since it shows the potential region of distribution when the formulation is applied to the skin or affected area. It is

performed by measuring the spreading diameter of 1 g of NEG between two horizontal glass plates (25 cm × 25 cm) while subjecting them to a weight of approximately 0.5 kg for a duration of 1 min [32].

#### 2.6.5. Drug Content

One gram of mupirocin-loaded NEG preparation was diluted with 100 mL of phosphate buffer and filtered through 0.45 micro-syringe filters. The drug content was measured using a spectrophotometric assay at  $\lambda_{\text{max}}$  of 222 nm. Using the same methodology, the drug content of the blank sample (sample devoid of drugs) was determined using the following equation:

$$\text{Percentage of drug content} = (\text{Actual/Theoretical}) \times 100$$

#### 2.7. The In Vitro Drug Release Study of NEG Formulation

In order to assess the in vitro release of mupirocin from the NEG formulation, the same approach as in Section 2.4.2 was used [28,33].

#### 2.8. Drug-Excipient Compatibility Studies (Fourier-Transform Infrared Spectroscopy (FTIR) Studies)

The infrared spectra were investigated using an FTIR spectrophotometer (FTIR spectrophotometer, SHIMADZU, IRAFFINITY-1S, Kyoto, Japan). The KBr pellet technique was used in which NE was poured on the KBr plate and dried via vacuum. All FTIR spectra were obtained between 4000 and 400  $\text{cm}^{-1}$ . The analysis was performed for the pure drug and formulations to detect any changes in the chemical structure [34].

#### 2.9. Scanning Electron Microscopy (SEM)

A microscopic method utilizing scanning electron microscopy (SEM) (JSM-6390LA, JEOL, Tokyo, Japan) was used to determine the morphology of the manufactured mupirocin-loaded NEG formula. Typically, a sputter coater was used to shield a slab with gold while a sample of the formulation was added and scanned. Next, using various magnifications, the morphology was detected at an acceleration voltage of 5 kV while operating under a reduced vacuum [26].

#### 2.10. Stability Study

Stability studies were used to evaluate the physical and chemical stabilities of the optimized mupirocin-loaded NEG formulation. According to recommendations from the International Conference on Harmonization (ICH), the sample was stored in a sealed plastic jar for 1 and 3 months under ambient ( $25 \pm 2$  °C/60 5% RH) and ( $5 \pm 3$  °C) conditions. At the prescribed time, the samples were examined for physical appearance, viscosity, spreadability, and in vitro release study [35].

#### 2.11. The Antibacterial Activity of Mupirocin-Loaded NEG against Different Bacterial Strains

In order to investigate the in vitro antibacterial activity of the optimized mupirocin-loaded NEG, an antibacterial examination was conducted using the disk diffusion method. The strain of MRSA bacterium (methicillin-resistant *Staphylococcus aureus*) used in the study was obtained from the American Type Culture Collection (ATCC). Basically, a sterile cork borer was used to create a 12 mm diameter disc in a Petri dish. Moller Hinton Agar, a bacterial culture medium, was present in the Petri dish. Each disk received a small amount of the investigated preparation in order to measure the diameter of the inhibition zone. The studied formulations were mupirocin-loaded NEG and NEG without mupirocin, compared with marketed mupirocin ointment (Bactroban<sup>®</sup>) as the control. The experiment was performed in triplicate with a mean value  $\pm$  SD. The plates were incubated for 24 h at 37 °C and then the zone of inhibition in each plate was measured and recorded [36].

### 2.12. Animals and Statement of Ethical Approval

The study was performed using 200–250 g adult male Wistar rats. The animals were kept in a pathogen-free environment with a 12 h day/night cycle and a temperature of 25 °C. In addition, regular pellet food was supplied, and they had unrestricted access to the water supply. The in vivo experiments were conducted in compliance with the ethical guidelines for animal use at King Faisal University. The Research Ethics Committee (REC) of King Faisal University (KFU-REC-2021- NOV-EA000134) provided its approval for the experiment's protocol.

### 2.13. Studies on Skin Irritation

For investigating skin irritancy, Wistar rats, adult males, weighing between 200 and 250 g, were used. Using a clipper, the animal's dorsal region was stripped of all hair one day before starting the investigation. On the hairless skin, each tested product was uniformly applied to an area of 4 cm<sup>2</sup> on the skin that was not covered with hair. After applying the formulation for 24, 48, and 72 h, the surface of the skin was checked for any indications of sensitivity, including erythema and edema. The observed sensitivity reaction was given a score of 0, 1, 2, or 3 depending on whether there was no reaction, a small reaction, or spotty or severe erythema, with or without edema [37].

### 2.14. The In Vivo Evaluation of Wound Healing Efficiency

#### 2.14.1. Design of the Experiment

Excision wound models were utilized in the current study for the evaluation of mupirocin-loaded NEG antibacterial activity. Four groups of rats were allocated, each containing four animals. Throughout the whole experiment, animals in all groups were screened daily for any wound contamination. None of the animal groups received an antibiotic and each group was treated only with the specified formula as follows:

- Group I: rats were kept to heal without treatment (control group);
- Group II: rats were given commercial ointment (50 mg);
- Group III: rats were given blank NEG (50 mg);
- Group IV: rats were given mupirocin-loaded NEG (50 mg of 2% NEG) [38].

#### 2.14.2. Excision Wound Establishment

Ketamine hydrochloride (50 mg/kg) and xylazine (10 mg/kg) were administered intraperitoneally to the rats to cause anesthesia [39]. The dorsal region of the anesthetized rats was first shaved and then sanitized with an alcohol swab before the wound was created. On the back of each animal, a 1 cm diameter, open cut, full-thickness wound was created employing a razor-sharp metal punch that was autoclave-sterilized. Due to the position of the wounds, the rats were unable to reopen them. Days of topical preparation administration began on day 0 and continued until the day of full wound healing. For the whole time of the experiment, daily topical applications of all preparations were made to the wound region starting on the day the excision wound was created. On days 0 through 21, wounds were left exposed to the air, and the wound healing ratio was assessed [40].

#### 2.14.3. Wound Area Measurement

On experiment days 0, 4, 7, and 14, digital photographs of the lesions were taken. Image J, version 1.45 (freeware; [rsbweb.nih.gov/ij/](https://rsbweb.nih.gov/ij/); Bethesda, MA, USA) was used to digitally quantify the lesion areas at predetermined periods. The images of the lesion regions were utilized to compute the percentage of wound area.

### 2.15. Statistical Analysis

All data were recorded as mean  $\pm$  standard deviation by applying Student's *t*-test and a one-way analysis of variance (ANOVA) test followed by the least significant difference (LSD) method as a post hoc test using SPSS statistics software, version 9 (IBM Corporation, Armonk, NY, USA). When the *p*-value < 0.05, the difference was considered to be significant.

### 3. Results

#### 3.1. Designing the Experiment

##### Fitting Models and Analyzing Statistical Data

As presented in Table 1, seventeen NE preparations were developed via a CCD approach using various concentrations of tea tree oil, Tween 80, and PEG 400. The different concentrations of the selected factors were examined for their influence on certain responses, namely the particle size and in vitro release. Statistical analysis of the data was performed using ANOVA in order to identify the model. As shown in Table 2, it was noticed that the best-fitting model for the  $Y_1$  response is the quadratic one, since it showed an  $R^2$  value of 0.9988 if compared with other models. However, the best fitting model for the  $Y_2$  response is the linear model since its  $R^2$  value was recorded as 0.9894 if compared with other models. Concerning the model F-value, it was detected to be 639.74 and 403.4 for  $Y_1$  and  $Y_2$ , respectively, demonstrating that the model is significant. Furthermore,  $p$ -values less than 0.05 indicate that the model terms are significant. In the case of the  $Y_1$  response, the model terms A, B, C, AB, AC, and  $A^2$  are significant; however, the model terms A, B, and C are significant for the  $Y_2$  reaction. Relating to the lack of fit value, it is essential for this parameter to be non-significant in order for the model to fit. It was recorded that the lack of fit was 3.78 and 0.895 with corresponding  $p$ -values of 0.2221 and 0.6378 for the two responses  $Y_1$  and  $Y_2$ , respectively. This result revealed a non-significant lack of fit.

**Table 2.** Statistical analysis of responses.

Source	$Y_1$		$Y_2$	
	F-Value	$p$ -Value	F-Value	$p$ -Value
<b>Model</b>	639.74	<0.0001 *	403.40	<0.0001 *
A	5245.74	<0.0001 *	1126.16	<0.0001 *
B	339.32	<0.0001 *	61.19	<0.0001 *
C	72.07	<0.0001 *	22.84	0.0004 *
AB	37.14	0.0005 *		
AC	12.21	0.0101 *		
BC	4.81	0.0643		
$A^2$	31.41	0.0008 *		
$B^2$	0.0157	0.9040		
$C^2$	3.60	0.0994		
Lack of fit	3.78	0.2221	0.8965	0.6378
$R^2$ analysis				
$R^2$		0.9988		0.9894
Adjusted $R^2$		0.9972		0.9869
Predicted $R^2$		0.9911		0.9820
Adequate precision		85.9518		62.9684
Model		Quadratic		Linear
Remark		Suggested		Suggested

A: Oil concentration; B: Tween 80 concentration; C: PEG 400;  $Y_1$ : particle size; and  $Y_2$ : in vitro release. \* Significant.

#### 3.2. The Characterization of Mupirocin-Loaded NE Formulations

##### 3.2.1. The Effect of Selected Factors on $Y_1$

The particle size of the developed formulations is a very significant factor to be assessed. Referring to Table 1, the particle sizes of all developed NEs along with their corresponding PDI values are displayed. The particle sizes of all NE formulations seemed to range from  $(97 \pm 2.0)$  to  $(375 \pm 4.5)$  nm. It was observable that using a higher concentration of tea tree oil would provide a formula with a larger particle size due to an increase in the dispersed phase [41]. On the contrary, a higher concentration of surfactant (B) would provide a smaller particle size while using the same oil concentration. This result was

ascribed to the relation between surfactant and interfacial tension since adding more surfactant would reduce the interfacial tension at the formula's interface and subsequently prevent the coalescence of particles and the formation of aggregates, keeping the particle size small [42]. On the same track, using a higher concentration of factor C, related to PEG 400, would lower the particle size upon using the same oil and surfactant concentration. Likewise, this finding could be attributed to the same fact concerning how surfactants and co-surfactants have a role in lowering interfacial tension, which would accordingly drop the particle size of the formulation [43].

In order to confirm the obtained results, the following mathematical equation was generated using the design approach, showing that particle size ( $Y_1$ ) was directly proportional to factor A, which was confirmed by the positive sign. On the other hand, the negative sign in front of factors B and C indicated an inverse relation between them and response  $Y_1$ .

$$Y_1 = 214.449 + 85.2714 * A - 21.6873 * B - 9.99492 * C - 9.375 * AB - 5.375 * AC + 3.375 * BC + 7.2625 * A^2 - 0.162123 * B^2 - 2.46022 * C^2$$

To further emphasize the attained data, several graphs were created using a CCD approach, which demonstrated the relation between all the selected factors and the observed particle size response  $Y_1$ . The substantial positive effect of factor (A) in addition to the negative effect of both factors B and C on the particle size response ( $Y_1$ ) is demonstrated clearly by the 3D-response surface plot as exhibited in Figure 1a–c. Moreover, the one-factor graph as plotted in Figure 2a–c explains the influence of each factor against the particle size response. The graph shows that response ( $Y_1$ ) related to the particle size of the developed formulations increased in relation to the increase in factor (A) concentration (Figure 1a); however, the response dropped upon increasing the other two factors B and C (Figure 1b,c).

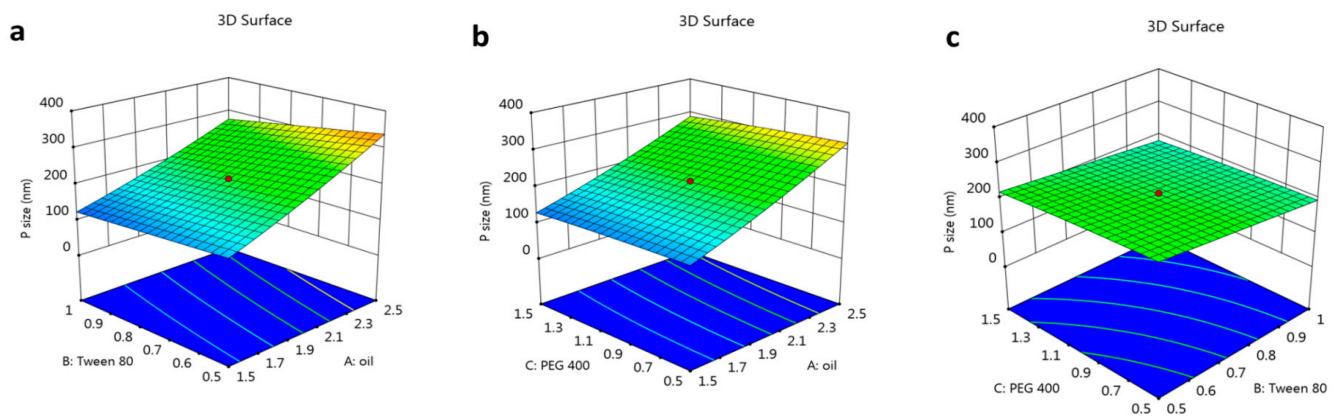


**Figure 1.** Three-dimensional response surface plots demonstrating the effect of factors (a) A and B, (b) A and C, and (c) B and C on particle size response ( $Y_1$ ).

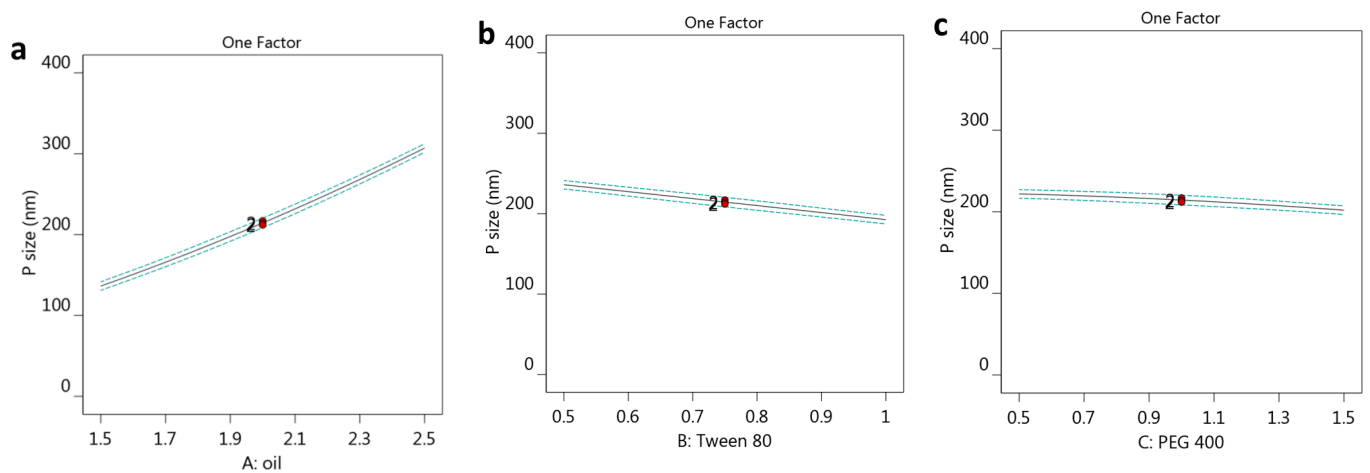


**Figure 2.** One factor plots representing (a) the influence of factor A, (b) the influence of factor B, and (c) the influence of factor C on particle size response  $Y_1$ .

Additionally, as per the data shown in Table 2, the adjusted and predicted  $R^2$  for the  $Y_1$  response were 0.9972 and 0.9911, respectively; these values seemed to be very close to each other since the difference between them is less than 0.2. This indicates that both values were in reasonable agreement with each other as seen in Figure 3a. Also, the adequate precision was (85.9518), which is an adequate signal that could navigate the design space.

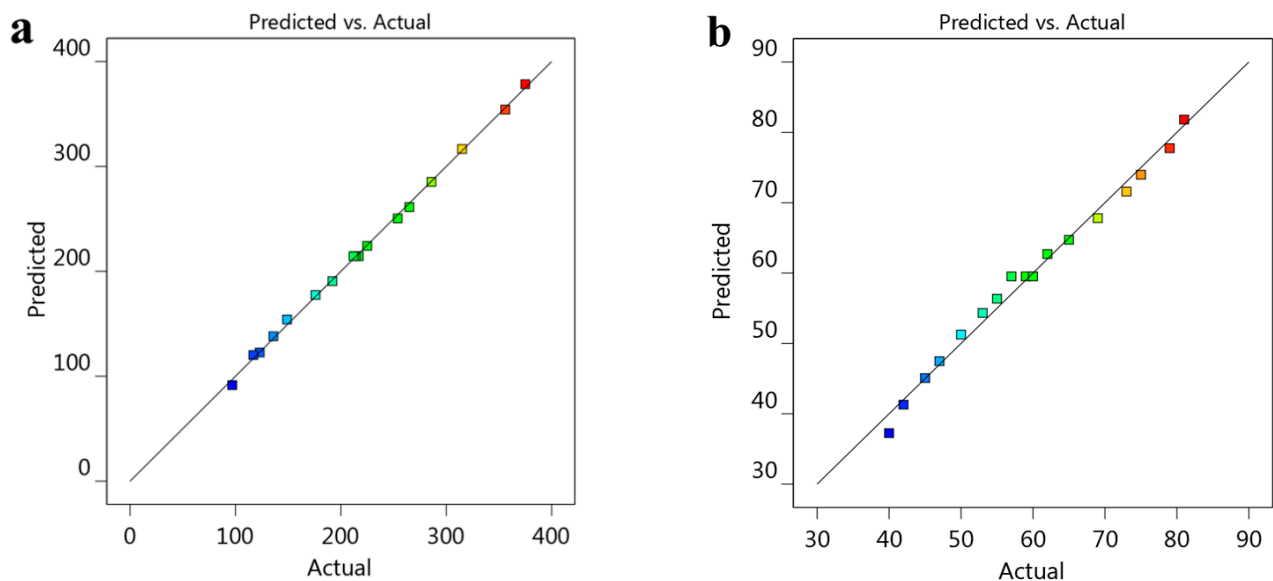


**Figure 3.** Linear correlation plots between actual and predicted values for (a) response  $Y_1$  and (b) response  $Y_2$ .

### 3.2.2. The Impact of Selected Factors on $Y_2$

The *in vitro* release study that represents the second factor ( $Y_2$ ) was evaluated for all formulations in order to determine the amount of mupirocin released over a period of 6 h. It is apparent in Table 1 that the percentage of mupirocin released ranged from  $40 \pm 3.0$  to  $81 \pm 4.0\%$ . Observing these data, the percentage of *in vitro* release decreased by increasing the tea tree oil concentration. This could be attributed to the higher particle size obtained by using a higher concentration of oil, which consequently provides a smaller surface area for the formula and permits a lower release of the drug [44]. On the other hand, it was noticed that even when the tea tree oil content was kept constant, increasing the surfactant concentration increased the percentage of mupirocin released. The reason

behind this result could relate to the decrease in the particle size and, consequently, cause an increase in the surface area that would enhance the percentage of in vitro release upon increasing the surfactant. The same finding was noticed upon using a co-surfactant, where a higher concentration of PEG400 improved the in vitro release study as well.

The established mathematical equation emphasizes all of the obtained results, where the negative sign in front of factor (A) indicates its antagonistic effect on  $Y_2$ . However, the positive sign served as confirmation of the synergistic influence of elements B and C. The generated equation is as follows:

$$Y_2 = 59.5294 - 13.25 * A + 3.08867 * B + 1.88715 * C$$

Additionally, the produced graphs from the CCD approach were very important for affirming the influence of the selected factors on the investigated in vitro release response  $Y_2$ . It is obvious based on the data in Figure 4a–c that the results were related to the 3D-response surface plot, the negative influence of factor (A), and the positive impact of factors (B and C) on the studied in vitro release response  $Y_2$ .

As well, it is apparent in Figure 5a–c that the one-factor plot was created to label the effect of all factors on the in vitro release response. It was validated that increasing the concentration of factor (A) resulted in a decrease in the in vitro release of the developed formulations. On the contrary, an increase in factors (B and C) exhibited a corresponding increase in the examined response.

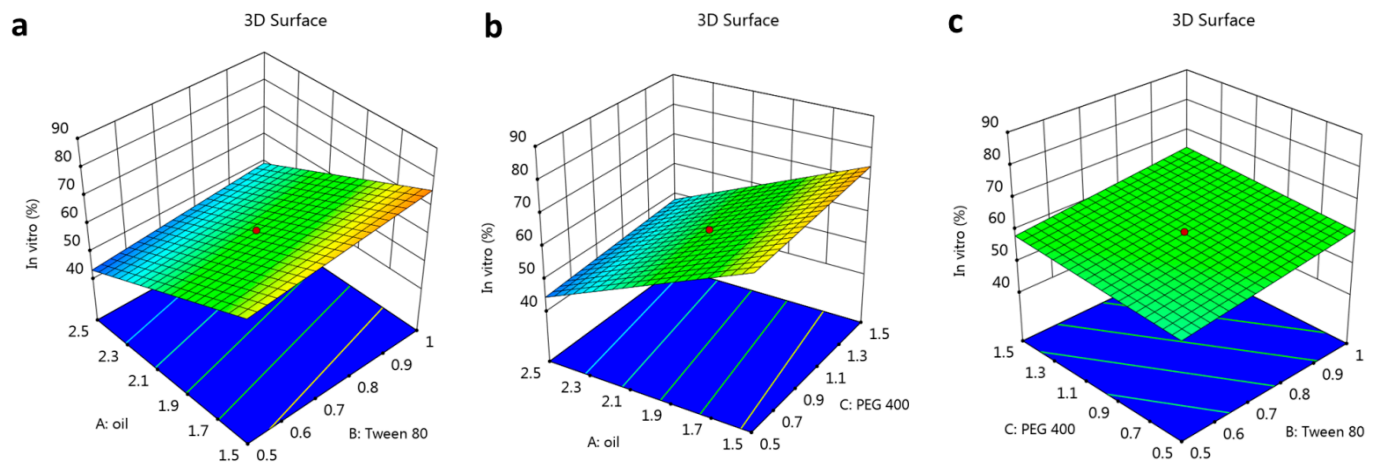


**Figure 4.** Three-dimensional response surface plots demonstrating the effect of factors (a) A and B, (b) A and C, and (c) B and C on the in vitro release response ( $Y_2$ ).

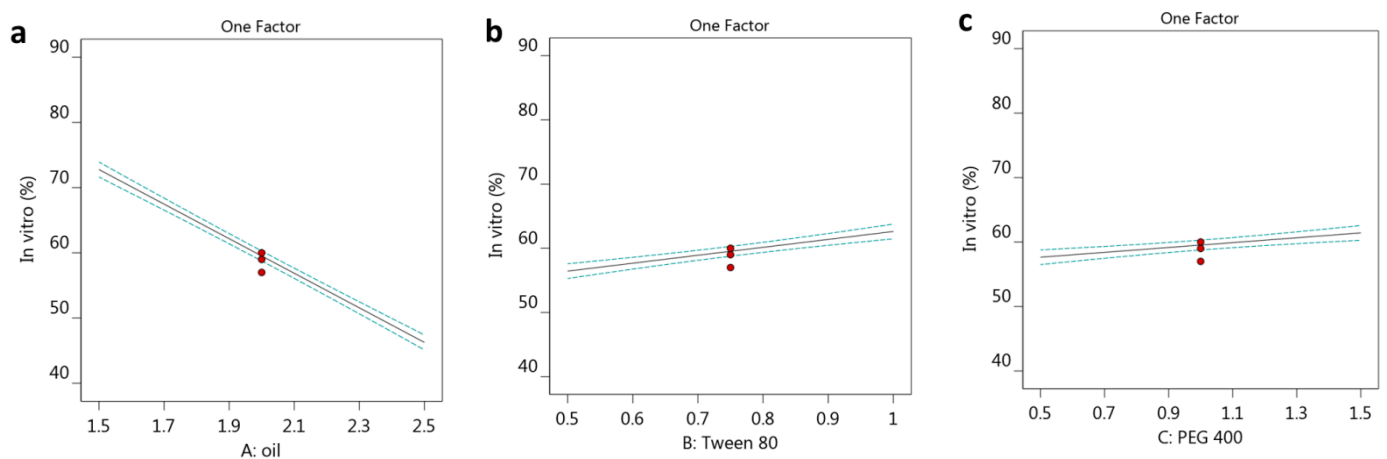


**Figure 5.** One factor plots representing (a) the influence of factor A, (b) the influence of factor B, and (c) the influence of factor C on the in vitro release response  $Y_2$ .

In addition, the linear relationship between adjusted and predicted  $R^2$  was emphasized as displayed in Table 2 and Figure 3b. Adjusted and predicted  $R^2$  values were 0.9869 and 0.9820, respectively, which refers to a reasonable match between both values since the difference between them was less than 0.2. Moreover, the value of adequate precision for the in vitro release response ( $Y_2$ ) was 62.9684, which is a required signal for navigating the design space.

### 3.3. Optimizing the Data

Several parameters could help in selecting the optimized formula depending on the numerical optimization, created graph models, and desirability function. The purpose was to direct the responses toward certain requisite objectives, which were to minimize the particle size, keep viscosity in range, and maximize the in vitro release of the drug from formulation. Based on the previous arrangement, the concentration of tea tree oil was oriented to be 1.5 g, Tween 80 was 1 g, and PEG 400 was 1.48 g as shown in Table 3 and Figure 6. These suggested amounts of selected factors provided the highest desirability value, which reached 0.918 as presented in Figure 6. The previous amounts were used to develop the optimized mupirocin NE formulation, which would be evaluated and compared with observed calculated values.

The fact that the predicted and observed values were remarkably close to one another was a prominent result. Figure 7 shows the particle size of the optimized mupirocin-loaded NE formulation of  $(125.0 \pm 3.6)$ . Additionally, its relative PDI value was  $0.204 \pm 0.27$ , in which the distribution of particle sizes enclosed within a small range of sizes is regarded as a positive indicator of stability [32].

**Table 3.** Predicted and observed values for the optimized mupirocin NE formulation.

Selected Factor	Constraint	
Tea tree oil concentration (g)	In range	
Tween 80 concentration (g)	In range	
PEG 400 concentration (g)	In range	
Response	Predicted values	Observed values
Particle size (nm)	$120.26 \pm 4.3$	$125.0 \pm 3.6$
In vitro release (%)	$77.75 \pm 1.45$	$75.86 \pm 1.5$

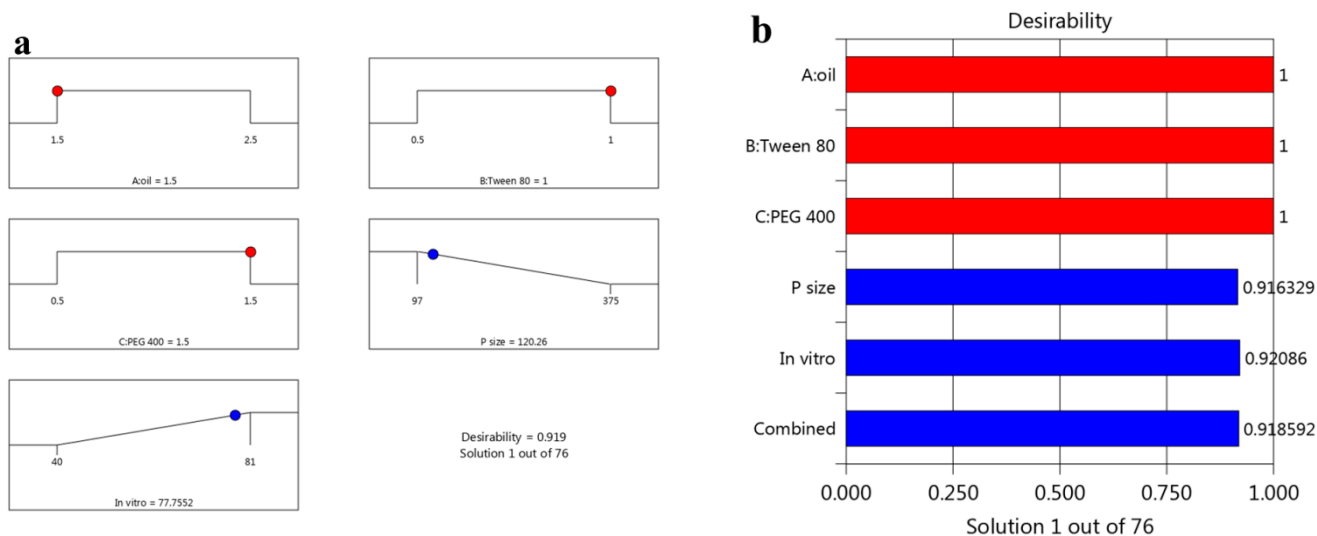


**Figure 6.** (a) Optimization ramps for the examined factors along with the predicted values of responses demonstrating the desirability value and (b) illustrating bar graphs with the desirability value.

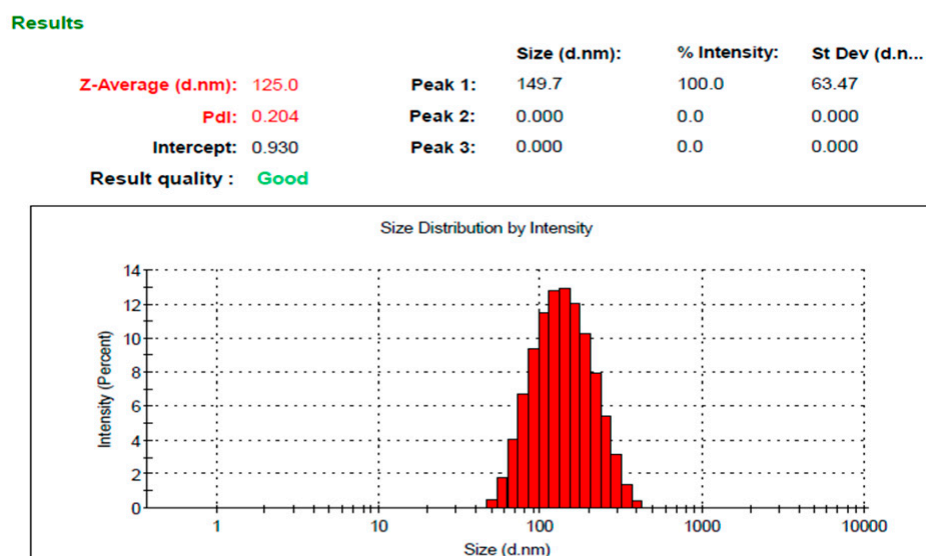


**Figure 7.** The particle size of the optimized mupirocin NE formulation.

### 3.4. The Characterization of the Optimized Mupirocin NE

#### 3.4.1. Visual Inspection

Visual examination of mupirocin-loaded NEG revealed that the preparation looked to be a smooth, uniform, and homogenous formulation showing a convenient physical appearance.

#### 3.4.2. pH Determination

Since it is very important for a topical formulation to show a pH value close to skin pH, measurement of this parameter was performed [45]. It was recorded that the pH of the formulated mupirocin-loaded NEG was  $6.13 \pm 0.25$ , which appears to be suitable to prevent any skin irritation and compatible with the pH of the skin.

#### 3.4.3. Viscosity Measurement

Viscosity is another vital parameter to be evaluated since it would affect the formulation behavior regarding the release of the drug from the formulations [46]. Accordingly, the viscosity of the studied mupirocin-loaded NEG formulation was evaluated and found to be  $19990 \pm 425.79$  cP, which appeared to be in the acceptable range for topical preparation.

#### 3.4.4. Spreadability Test

In addition, spreadability is also essential to determine for topical preparation where a lower value of spreadability indicates easier application over the skin [47]. As a result, the spreadability of mupirocin-loaded NEG formulation was measured and found to be  $48.8 \pm 2.7$  mm, which indicates an adequate result for a topical preparation to be readily applied over the skin.

#### 3.4.5. Drug Content

An evaluation of the drug content was performed and appeared to be over  $99.26 \pm 0.5\%$ , suggesting that the mupirocin was distributed evenly throughout the preparations.

### 3.5. The In Vitro Drug Release Study of NEG Formulation

The outline of the in vitro release of mupirocin from the mupirocin-based NEG formulation was estimated over a period of 6 h and compared with the release from the NE as depicted in Figure 8. It was quite clear that the release of mupirocin from the NEG formulation ( $51.4 \pm 4.7\%$ ) and from the optimized NE ( $75.86 \pm 1.5\%$ ) differed significantly ( $p < 0.05$ ). It was documented earlier that the in vitro release of the drug from the prepara-

tion would be significantly influenced by the inclusion of a gelling agent in the formulation that would provide higher viscosity [48]. Therefore, the percentage of drug in vitro release from more viscous preparations was actually decreased [49]. In spite of showing a larger percentage of mupirocin release from the NE formulation, the mupirocin-based NEG is considered to be the best due to its adequate viscosity and proper spreadability, which enables easier and more effective application to the affected area [50].

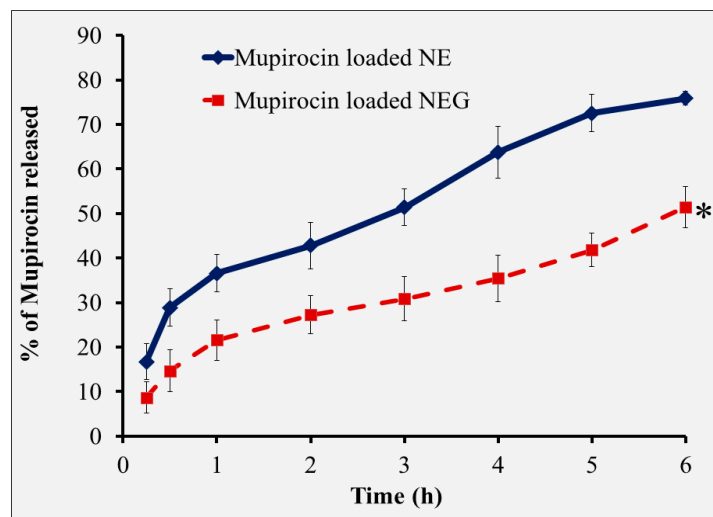


**Figure 8.** Profile of in vitro release of mupirocin from the optimized NE and NEG formulations in phosphate buffer pH 5.5 at 32 °C. The results from three experiments are presented as mean  $\pm$  SD. \*  $p < 0.05$  compared with mupirocin-loaded NE.

### 3.6. FTIR (Fourier-Transform Infrared Spectroscopy) Study

Infrared spectroscopy was utilized to explore any chemical interactions between the drug and any other substances included in the formulation as shown in Figure 9. The spectra exhibited distinctive peaks for mupirocin, blank mupirocin, and mupirocin-loaded NEG. Observed spectra of pure mupirocin corresponding to the major peaks were found at  $3480\text{ cm}^{-1}$  (O-H),  $3309\text{ cm}^{-1}$ ,  $2934\text{ cm}^{-1}$  (alkyl C-H),  $1729\text{ cm}^{-1}$ ,  $1712\text{ cm}^{-1}$  (C=O),  $1231\text{ cm}^{-1}$ , and  $1222\text{ cm}^{-1}$  (C-O). Upon observing the FTIR spectra for Blank-NEG and mupirocin NEG, it was found that there is strong broadband around  $3300\text{ cm}^{-1}$  due to O-H stretching that results from intermolecular hydrogen. Furthermore, the existence of a distinctive peak between  $1700$  and  $1500\text{ cm}^{-1}$  in both mupirocin NEG and blank NEG formulations suggested that the peaks of mupirocin and tea tree oil overlapped. This demonstrated that mupirocin was successfully trapped within the tea tree oil without any indication of a major chemical interaction between the drug and the oil. This result was consistent with Alhasso et al. who stated that there were no interactions or interferences between the inclusion of mupirocin and the essential oil nanoemulsion [51].

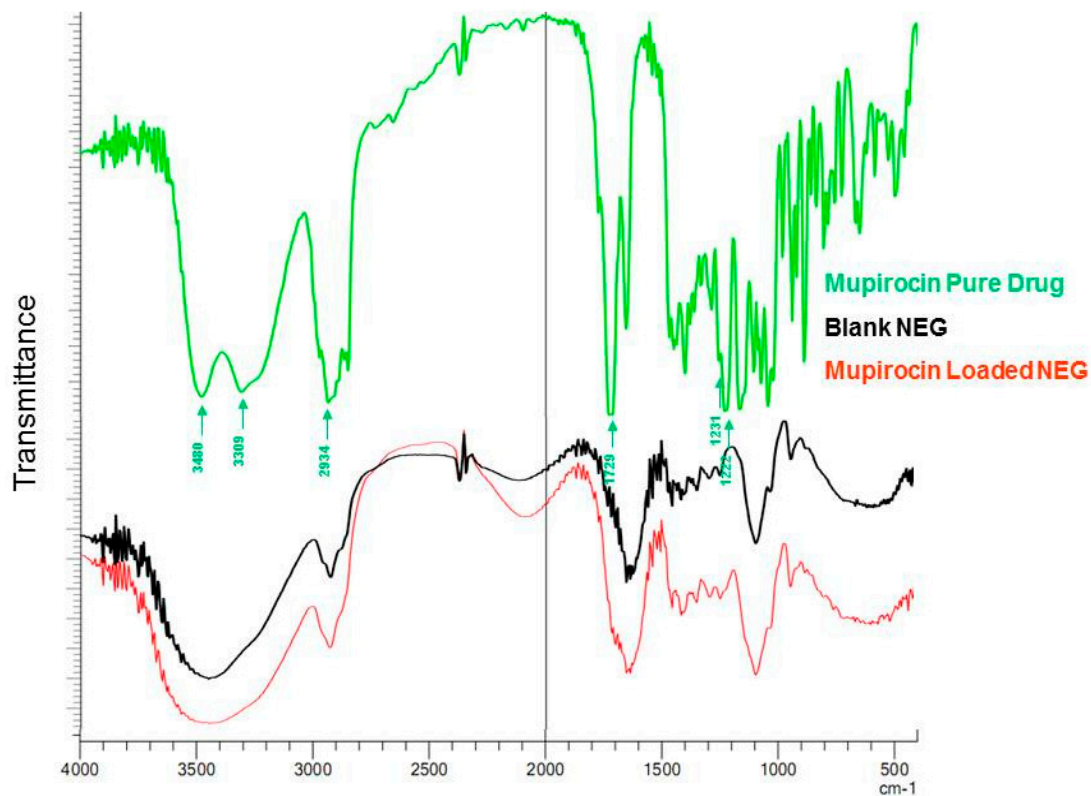


**Figure 9.** FTIR spectra of pure mupirocin, blank NEG, and mupirocin-loaded NEG.

### 3.7. Scanning Electron Microscopy (SEM)

As exhibited in Figure S1, the surface morphology of the developed mupirocin-loaded NEG formulation was performed using a scanning electron microscope. Discrete spherical vesicles were disseminated, without aggregating, through the gel substrate as a network, which suggested the formation of the nanoemulgel.

### 3.8. Stability Study

As depicted in Figure 10, checking for mupirocin-based NEG stability was conducted relative to specific evaluated parameters including physical inspection, pH, viscosity, spreadability, and in vitro release behavior. The study was performed by comparing stored samples with fresh NEG formulation following storage for 3 months at variant conditions. Obviously, the formulation showed no change in color, odor, or homogeneity, and no phase separation was detected during the entire period of storage. Additionally, non-significant variations were detected in all evaluated parameters for mupirocin-based NEG formulation following 3 months of storage at conditions of 4 °C and 25 °C when compared with freshly prepared NEG preparation ( $p < 0.05$ ). This study highlights the formulation's stability and validates NEG as a powerful drug carrier.

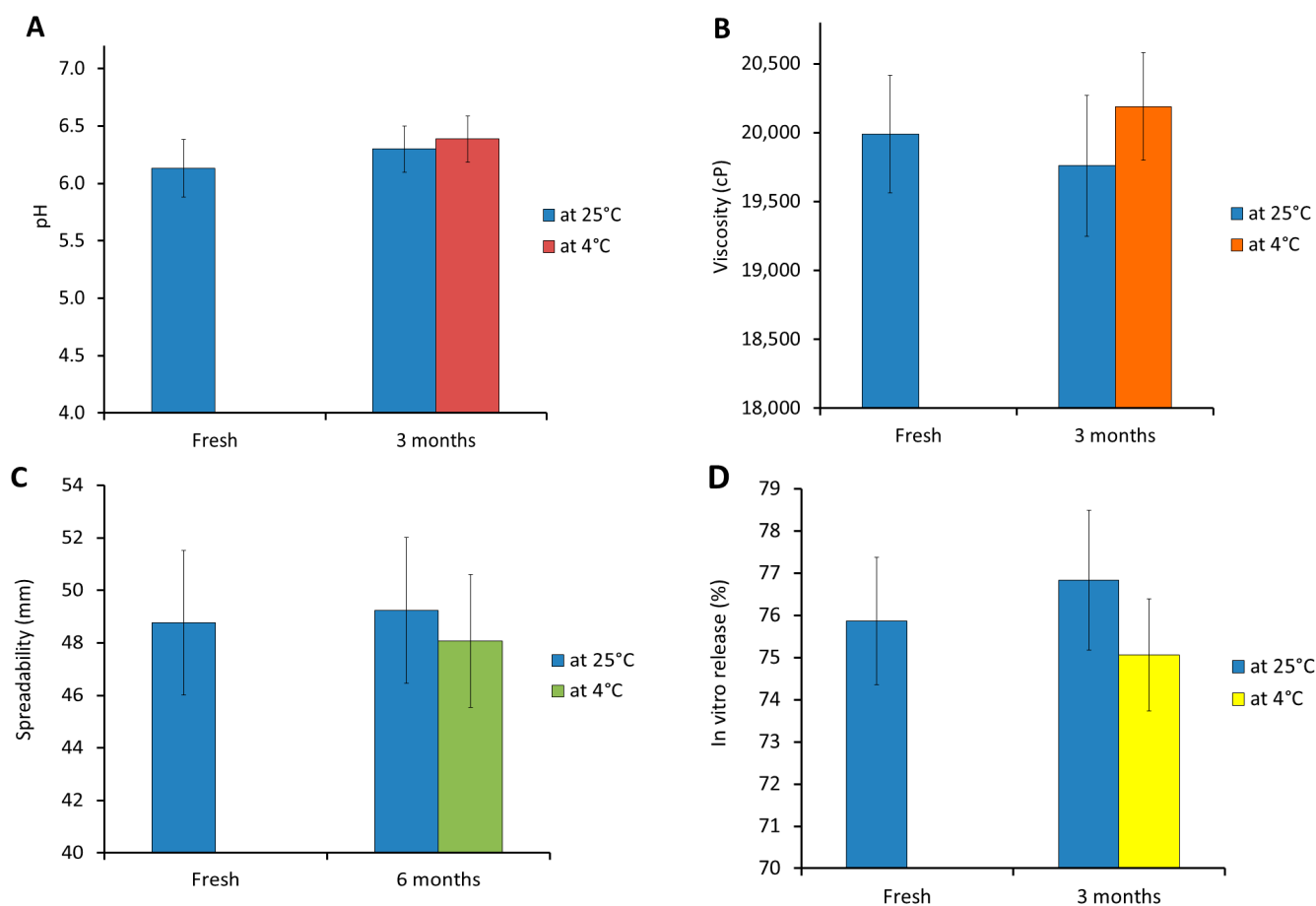


**Figure 10.** Stability study outline for mupirocin-loaded NEG formulation investigated at 4 °C and 25 °C for 3 months in terms of (A) pH, (B) viscosity, (C) spreadability, and (D) in vitro release compared with freshly prepared NEG formulation.

### 3.9. The Antibacterial Activity of Mupirocin-Loaded NEG against MRSA Bacterial Strain

The efficacy of mupirocin formulation against MRSA was estimated by performing the disc diffusion method. As previously mentioned, the investigation was carried out utilizing several formulations, specifically mupirocin NEG, blank NEG, and marketed Bactroban® ointment. The investigation depended on measuring the diameter of the inhibition zone created by the tested formulations due to their effectiveness against the bacteria, as shown in Table 4 and Figure 11. It was observed that mupirocin-loaded NEG had a significant antibacterial impact on the cultivated bacteria. This is, in fact, because mupirocin-loaded NEG formulations were shown to produce inhibition zones with diameters that were much larger than those produced by blank NEG and commercially available products ( $p < 0.05$ ). Nevertheless, it was remarked that blank NEG produced with tea tree oil showed a significant inhibition of bacterial development, which was undoubtedly attributed to the tea tree oil's antibacterial activity. In fact, it was previously confirmed that tea tree oil has considerable antimicrobial activity against a wide range of bacteria [52]. This behavior is reportedly due to the main content of tea tree oil, which is principally terpinen-4-ol [26]. Conclusively, and based on the obtained results, the greater antimicrobial activity exhibited by mupirocin-loaded NEG could be attributed to the integration of mupirocin and tea tree oil, which resulted in improving the antibacterial activity of mupirocin. In fact, this result emphasizes previous conclusions regarding the problem of bacterial resistance where a combination therapy-based treatment approach was thought to significantly increase the antibacterial activity of several antibiotics [53]. Therefore, mupirocin-loaded NEG might help in managing the problem of MRSA infections, which has been getting worse because

of the inappropriate use of mupirocin for treating skin infections, and which has led to the emergence of mupirocin resistance [54].

**Table 4.** Antibacterial activity of examined formulations against MRSA bacterial strain.

Inhibition Zone Diameter (cm)	Bacterial Strain
	MRSA
Blank NEG	1.8 ± 0.10
Bactroban® ointment	3.0 ± 0.15 *
Mupirocin-loaded NEG	3.4 ± 0.15 * °

Values are shown as mean ± SD; \* ( $p < 0.05$ ) compared with blank NEG; and ° ( $p < 0.05$ ) compared with marketed mupirocin (Bactroban® ointment).

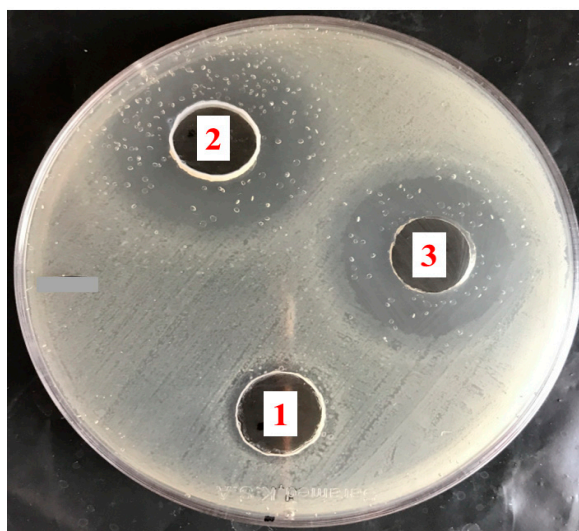


**Figure 11.** Inhibition zone diameter caused by studied formulations: (1) blank NEG; (2) mupirocin-loaded NEG; and (3) Bactroban® ointment on MRSA bacterial strain.

### 3.10. Studies on Skin Irritation

Observations were made to determine if the back skin of rats given mupirocin-loaded NEG formula showed any signs of irritation. Remarkably, throughout the entire investigation period, no irritation, erythema, or edema could be seen in the area under examination. This outcome demonstrated that the formulations were safe for topical application.

### 3.11. The In Vivo Evaluation of Wound Healing Efficiency

The effectiveness of in vivo wound healing was evaluated by determining the reduction in wound area, which is considered a sign of healing. Descriptive photographs were taken of the wound area on different days, starting with the day of wound creation (day 0) and on days 4, 7, 14, and 21 after the wound was created. As exhibited in Table 5 and Figure 12, for each group in the study, demonstrative wound shots were taken on different days in order to assess the probable healing of the treated formulations in wounded animals. Primarily, on the first day after the wound creation, a bright red color was perceived in all wounds, indicating the recovery of the blood to form blood clotting at the underlying muscle after the skin injury. There was a non-significant difference in wound contraction size between all treated groups under study. On the fourth day following wound formation, noticeable new skin started to appear in group IV treated animals, indicating the start of the wound healing stage. However, no discernible distinction was seen between any of the other treated groups. On the seventh day following wound formation, a dark brown color was noticed for all treated animal groups, indicating scab formation. However, the wound in the untreated control group was still marginally red and inflamed. A significant

difference was detected between the mupirocin-loaded NEG-treated group and the marketed ointment-treated group ( $p < 0.05$ ). Additionally, there was a significant difference between the marketed ointment-treated group and the blank NEG-treated group ( $p < 0.05$ ). Regarding the untreated control group, it was obvious that the wound was still inflamed, with a slight red color. Moreover, on the fourteenth day subsequent to wound creation, the mupirocin-loaded NEG-treated animal group displayed a significantly reduced wound size when compared with other animal groups ( $p < 0.05$ ). Afterward, 21 days post-wound formation, the mupirocin-loaded NEG-treated group showed a more significant reduction in wound area that seemed to be close to complete healing compared with other groups that received either the marketed ointment or the blank NEG formulation. On the other hand, the untreated control group still exhibited an unhealed open wound. The findings demonstrate the efficiency of mupirocin-loaded NEG in wound healing. This result appeared to be due to the synergistic action between mupirocin and tea tree oil that helps to provide more enhanced and rapid wound closure, which was found to be significant compared with other groups under investigation ( $p < 0.05$ ). This result was in accordance with Gangwar et al., who suggested the importance of sticking to a novel strategy to enhance the efficiency of mupirocin by combining it with other antimicrobial agents or natural products [55].

Day	Control Un-treated	Marketed ointment	Blank Mupirocin	Mupirocin loaded NEG
0 day				
4th day				
7th day				
14th day				

**Figure 12.** Photographic illustration demonstrating the influence of investigated topical formulations on wound healing in animals on various days after the formation of an excision wound.

**Table 5.** Percentage of unhealed wound lesions at various periods in different examination groups.

Days	% of Unhealed Wound Lesions			
	Control Untreated	Marketed Ointment	Blank NEG	Mupirocin-Loaded NEG
0	102.8 ± 4.7	101 ± 5.3	102.8 ± 5.7	102.8 ± 5.7
4	97.3 ± 5.1	73.3 ± 1.4 * °	80 ± 4.0 * \$	61.63 ± 3.2 * ° \$
7	94.0 ± 4.5	54.3 ± 3.4 * °	72.53 ± 1.53 * \$	31.67 ± 5.1 * ° \$
14	90.3 ± 4.5	36.67 ± 3.0 * °	50.0 ± 1.0 * \$	10.27 ± 2.0 * ° \$

All data are shown as mean ± SD ( $n = 4$ ). \* Specifies significantly different from the control untreated group; ° specifies significantly different from blank NEG-treated group; and \$ indicates significantly different from the marketed ointment-treated group ( $p < 0.05$ ).

#### 4. Conclusions

In conclusion, a nanoemulsion preparation using tea tree oil was developed and optimized using a central composite design. The optimized nanoemulsion was well integrated into the gel base to form a nanoemulgel formulation for the topical delivery of mupirocin. Mupirocin-loaded nanoemulgel was successfully evaluated for its characteristics to verify its suitability for topical application. Afterward, the formulation was evaluated for its antibacterial activity and proved to be active against MRSA, providing a large inhibition zone that was promoted by the antibacterial effect of tea tree oil. Ultimately, the wound healing activity of mupirocin-loaded nanoemulgel was evaluated on excision wound models and provided good healing for the wound. However, further investigation of wound healing in animals infected with different bacterial strains should be considered in the future. This study emphasized that the antibacterial and wound healing efficiencies of mupirocin are potentiated, especially when integrated with tea tree oil. Additionally, the nanoemulgel was demonstrated to be the nanocarrier of choice for the topical delivery of drugs.

**Supplementary Materials:** The following supporting information can be downloaded at: <https://www.mdpi.com/article/10.3390/app132413244/s1>, Figure S1: Morphological screening of the developed Mupirocin loaded NEG formulation using scanning electron microscopy.

**Author Contributions:** Conceptualization, M.M.B. and H.S.E.; methodology, M.M.B. and H.S.E.; software, H.S.E.; validation, H.S.E., T.M.S. and W.E.S.; formal analysis, M.M.B.; investigation, M.M.B.; resources, T.M.S.; data curation, M.M.B.; writing—original draft preparation, M.M.B. and H.S.E.; writing—review and editing, T.M.S.; visualization, H.S.E. and W.E.S.; supervision, T.M.S.; project administration, M.M.B. and H.S.E.; and funding acquisition, T.M.S. All authors have read and agreed to the published version of the manuscript.

**Funding:** This research was funded by the Deanship of Scientific Research, Vice Presidency for Graduate Studies and Scientific Research, King Faisal University, Saudi Arabia, grant number 4,359, and the APC was funded by the Deanship of Scientific Research, Vice Presidency for Graduate Studies and Scientific Research, King Faisal University, Saudi Arabia, Al-Ahsaa, KSA, grant number 4,359.

**Institutional Review Board Statement:** This study was conducted in accordance with the Declaration of Helsinki and approved by the Institutional Review Board (or Ethics Committee) of King Faisal University (KFU-REC-2021- NOV-EA000134).

**Informed Consent Statement:** Not applicable.

**Data Availability Statement:** Data are contained within the article and supplementary materials.

**Acknowledgments:** The authors acknowledge the Deanship of Scientific Research, Vice Presidency for Graduate Studies and Scientific Research, King Faisal University, Saudi Arabia for the financial support and also acknowledge the College of Clinical Pharmacy for the provision of lab facilities.

**Conflicts of Interest:** The authors declare no conflict of interest.

## References

1. Connolly, J.A.; Wilson, A.; Macioszek, M.; Song, Z.; Wang, L.; Mohammad, H.H.; Yadav, M.; di Martino, M.; Miller, C.E.; Hothersall, J. Defining the genes for the final steps in biosynthesis of the complex polyketide antibiotic mupirocin by *Pseudomonas fluorescens* NCIMB10586. *Sci. Rep.* **2019**, *9*, 1542. [[CrossRef](#)] [[PubMed](#)]
2. David, S.R.; Malek, N.; Mahadi, A.H.; Chakravarthi, S.; Rajabalaya, R. Development of controlled release silicone adhesive-based mupirocin patch demonstrates antibacterial activity on live rat skin against *Staphylococcus aureus*. *Drug Des. Dev. Ther.* **2018**, *12*, 481–494. [[CrossRef](#)]
3. Twilley, D.; Reva, O.; Meyer, D.; Lall, N. Mupirocin Promotes Wound Healing by Stimulating Growth Factor Production and Proliferation of Human Keratinocytes. *Front. Pharmacol.* **2022**, *13*, 862112. [[CrossRef](#)] [[PubMed](#)]
4. Verma, V.; Kaushik, D. Mupirocin Mounted copper nanoparticle offered augmented drug delivery against resistant bacteria. *Indian J. Pharm. Educ. Res.* **2020**, *54*, 637–646. [[CrossRef](#)]
5. Shehata, T.M.; Elsewedy, H.S. Paclitaxel and myrrh oil combination therapy for enhancement of cytotoxicity against breast cancer; QbD approach. *Processes* **2022**, *10*, 907. [[CrossRef](#)]
6. Sharmeen, J.B.; Mahomoodally, F.M.; Zengin, G.; Maggi, F. Essential Oils as Natural Sources of Fragrance Compounds for Cosmetics and Cosmeceuticals. *Molecules* **2021**, *26*, 666. [[CrossRef](#)] [[PubMed](#)]
7. Carson, C.F.; Hammer, K.A.; Riley, T.V. *Melaleuca alternifolia* (Tea Tree) oil: A review of antimicrobial and other medicinal properties. *Clin. Microbiol. Rev.* **2006**, *19*, 50–62. [[CrossRef](#)]
8. Corona-Gómez, L.; Hernández-Andrade, L.; Mendoza-Elvira, S.; Suazo, F.M.; Ricardo-González, D.I.; Quintanar-Guerrero, D. In vitro antimicrobial effect of essential tea tree oil (*Melaleuca alternifolia*), thymol, and carvacrol on microorganisms isolated from cases of bovine clinical mastitis. *Int. J. Vet. Sci. Med.* **2022**, *10*, 72–79. [[CrossRef](#)]
9. Trombetta, D.; Castelli, F.; Sarpietro, M.G.; Venuti, V.; Cristani, M.; Daniele, C.; Saija, A.; Mazzanti, G.; Bisignano, G. Mechanisms of antibacterial action of three monoterpenes. *Antimicrob. Agents Chemother.* **2005**, *49*, 2474–2478. [[CrossRef](#)]
10. Yadav, E.; Kumar, S.; Mahant, S.; Khatkar, S.; Rao, R. Tea tree oil: A promising essential oil. *J. Essent. Oil Res.* **2017**, *29*, 201–213. [[CrossRef](#)]
11. Tan, C.; McClements, D.J. Application of advanced emulsion technology in the food industry: A review and critical evaluation. *Foods* **2021**, *10*, 812. [[CrossRef](#)] [[PubMed](#)]
12. Nasr, A.M.; Aboelenin, S.M.; Alfaifi, M.Y.; Shati, A.A.; Elbehairi, S.E.I.; Elshaarawy, R.F.; Elwahab, N.H.A. Quaternized Chitosan Thiol Hydrogel-Thickened Nanoemulsion: A Multifunctional Platform for Upgrading the Topical Applications of Virgin Olive Oil. *Pharmaceutics* **2022**, *14*, 1319. [[CrossRef](#)] [[PubMed](#)]
13. Shehabeldine, A.M.; Doghish, A.S.; El-Dakrouy, W.A.; Hassanin, M.M.H.; Al-Askar, A.A.; AbdElgawad, H.; Hashem, A.H. Antimicrobial, Antibiofilm, and Anticancer Activities of *Syzygium aromaticum* Essential Oil Nanoemulsion. *Molecules* **2023**, *28*, 5812. [[CrossRef](#)] [[PubMed](#)]
14. Marwa, A.; Iskandarsyah; Jufri, M. Nanoemulsion curcumin injection showed significant anti-inflammatory activities on carrageenan-induced paw edema in Sprague-Dawley rats. *Heliyon* **2023**, *9*, e15457. [[CrossRef](#)] [[PubMed](#)]
15. Guo, X.; Zhang, J.; Liu, X.; Lu, Y.; Shi, Y.; Li, X.; Wang, S.; Huang, J.; Liu, H.; Zhou, H.; et al. Antioxidant nanoemulsion loaded with latanoprost enables highly effective glaucoma treatment. *J. Control. Release* **2023**, *361*, 534–546. [[CrossRef](#)] [[PubMed](#)]
16. Yen, C.C.; Chen, Y.C.; Wu, M.T.; Wang, C.C.; Wu, Y.T. Nanoemulsion as a strategy for improving the oral bioavailability and anti-inflammatory activity of andrographolide. *Int. J. Nanomed.* **2018**, *13*, 669–680. [[CrossRef](#)] [[PubMed](#)]
17. Monge, C.; Stoppa, I.; Ferraris, C.; Bozza, A.; Battaglia, L.; Cangemi, L.; Miglio, G.; Pizzimenti, S.; Clemente, N.; Gigliotti, C.L. Parenteral Nanoemulsions Loaded with Combined Immuno-and Chemo-Therapy for Melanoma Treatment. *Nanomaterials* **2022**, *12*, 4233. [[CrossRef](#)]
18. Rai, V.K.; Mishra, N.; Yadav, K.S.; Yadav, N.P. Nanoemulsion as pharmaceutical carrier for dermal and transdermal drug delivery: Formulation development, stability issues, basic considerations and applications. *J. Control. Release* **2018**, *270*, 203–225. [[CrossRef](#)]
19. Krishnan, V.; Mitragotri, S. Nanoparticles for topical drug delivery: Potential for skin cancer treatment. *Adv. Drug Deliv. Rev.* **2020**, *153*, 87–108. [[CrossRef](#)]
20. Tapfumaneyi, P.; Imran, M.; Mohammed, Y.; Roberts, M.S. Recent advances and future prospective of topical and transdermal delivery systems. *Front. Drug Deliv.* **2022**, *2*, 957732. [[CrossRef](#)]
21. Makvandi, P.; Caccavale, C.; Della Sala, F.; Zeppetelli, S.; Veneziano, R.; Borzacchiello, A. Natural Formulations Provide Antioxidant Complement to Hyaluronic Acid-Based Topical Applications Used in Wound Healing. *Polymers* **2020**, *12*, 1847. [[CrossRef](#)] [[PubMed](#)]
22. Donthi, M.R.; Munnangi, S.R.; Krishna, K.V.; Saha, R.N.; Singhvi, G.; Dubey, S.K. Nanoemulgel: A Novel Nano Carrier as a Tool for Topical Drug Delivery. *Pharmaceutics* **2023**, *15*, 164. [[CrossRef](#)] [[PubMed](#)]
23. Choudhury, H.; Gorain, B.; Pandey, M.; Chatterjee, L.A.; Sengupta, P.; Das, A.; Molugulu, N.; Kesharwani, P. Recent Update on Nanoemulgel as Topical Drug Delivery System. *J. Pharm. Sci.* **2017**, *106*, 1736–1751. [[CrossRef](#)]
24. Debnath, S.; Aishwarya, M.; Babu, M.N. Formulation by design: An approach to designing better drug delivery systems. *Pharma Times* **2018**, *50*, 9–14.
25. Nainggolan, E.A.; Banout, J.; Urbanova, K. Application of Central Composite Design and Superimposition Approach for Optimization of Drying Parameters of Pretreated Cassava Flour. *Foods* **2023**, *12*, 2101. [[CrossRef](#)]

26. Elsewedy, H.S.; Shehata, T.M.; Soliman, W.E. Tea Tree Oil Nanoemulsion-Based Hydrogel Vehicle for Enhancing Topical Delivery of Neomycin. *Life* **2022**, *12*, 1011. [[CrossRef](#)] [[PubMed](#)]
27. Shehata, T.M.; Almostafa, M.M.; Elsewedy, H.S. Development and Optimization of Nigella sativa Nanoemulsion Loaded with Pioglitazone for Hypoglycemic Effect. *Polymers* **2022**, *14*, 3021. [[CrossRef](#)]
28. Elsewedy, H.S.; Younis, N.S.; Shehata, T.M.; Mohamed, M.E.; Soliman, W.E. Enhancement of anti-inflammatory activity of optimized niosomal colchicine loaded into jojoba oil-based emulgel using response surface methodology. *Gels* **2021**, *8*, 16. [[CrossRef](#)]
29. Donthi, M.R.; Saha, R.N.; Singhvi, G.; Dubey, S.K. Dasatinib-Loaded Topical Nano-Emulgel for Rheumatoid Arthritis: Formulation Design and Optimization by QbD, In Vitro, Ex Vivo, and In Vivo Evaluation. *Pharmaceutics* **2023**, *15*, 736. [[CrossRef](#)]
30. Razzaq, F.A.; Asif, M.; Asghar, S.; Iqbal, M.S.; Khan, I.U.; Khan, S.-U.-D.; Irfan, M.; Syed, H.K.; Khames, A.; Mahmood, H. Glimepiride-loaded nanoemulgel; development, in vitro characterization, ex vivo permeation and in vivo antidiabetic evaluation. *Cells* **2021**, *10*, 2404. [[CrossRef](#)]
31. Zaki, N.M.; Awad, G.A.; Mortada, N.D.; Abd ElHady, S.S. Enhanced bioavailability of metoclopramide HCl by intranasal administration of a mucoadhesive in situ gel with modulated rheological and mucociliary transport properties. *Eur. J. Pharm. Sci.* **2007**, *32*, 296–307. [[CrossRef](#)]
32. Elsewedy, H.S.; Shehata, T.M.; Soliman, W.E. Shea Butter Potentiates the Anti-Bacterial Activity of Fusidic Acid Incorporated into Solid Lipid Nanoparticle. *Polymers* **2022**, *14*, 2436. [[CrossRef](#)] [[PubMed](#)]
33. Salamanca, C.H.; Barrera-Ocampo, A.; Lasso, J.C.; Camacho, N.; Yarce, C.J. Franz diffusion cell approach for pre-formulation characterisation of ketoprofen semi-solid dosage forms. *Pharmaceutics* **2018**, *10*, 148. [[CrossRef](#)] [[PubMed](#)]
34. Ojo, O.E.; Ilomuanya, M.O.; Sekunowo, O.I.; Gbenebor, O.P.; Adeosun, S.O. Development and characterization of mupirocin encapsulated in animal bone-derived hydroxyapatite for management of chronic wounds. *Beni-Suef Univ. J. Basic Appl. Sci.* **2022**, *11*, 82. [[CrossRef](#)]
35. Elsewedy, H.S.; Shehata, T.M.; Almostafa, M.M.; Soliman, W.E. Hypolipidemic activity of olive oil-based nanostructured lipid carrier containing atorvastatin. *Nanomaterials* **2022**, *12*, 2160. [[CrossRef](#)] [[PubMed](#)]
36. Nathan, P.; Law, E.J.; Murphy, D.F.; MacMillan, B.G.J.B. A laboratory method for selection of topical antimicrobial agents to treat infected burn wounds. *Burns* **1978**, *4*, 177–187. [[CrossRef](#)]
37. Si, S.; Swain, S.; Kanungo, S.; Gupta, R. Preparation and evaluation of gels from gum of Moringa oleifera. *Indian J. Pharm. Sci.* **2006**, *68*, 777.
38. Kamlungmak, S.; Nakpheng, T.; Kaewpaiboon, S.; Mudhar Bintang, M.A.K.; Prom-In, S.; Chunchachaichana, C.; Suwandecha, T.; Srichana, T. Safety and Biocompatibility of Mupirocin Nanoparticle-Loaded Hydrogel on Burn Wound in Rat Model. *Biol. Pharm. Bull.* **2021**, *44*, 1707–1716. [[CrossRef](#)]
39. Chollet, J.L.; Jozwiakowski, M.J.; Phares, K.R.; Reiter, M.J.; Roddy, P.J.; Schultz, H.J.; Ta, Q.V.; Tomai, M.A. Development of a topically active imiquimod formulation. *Pharm. Dev. Technol.* **1999**, *4*, 35–43. [[CrossRef](#)]
40. Quazi, A.; Patwekar, M.; Patwekar, F.; Mezni, A.; Ahmad, I.; Islam, F. Evaluation of Wound Healing Activity (Excision Wound Model) of Ointment Prepared from Infusion Extract of Polyherbal Tea Bag Formulation in Diabetes-Induced Rats. *Evid. -Based Complement. Altern. Med. ECAM* **2022**, *2022*, 1372199. [[CrossRef](#)]
41. Wróblewska, M.; Szymańska, E.; Winnicka, K. The Influence of Tea Tree Oil on Antifungal Activity and Pharmaceutical Characteristics of Pluronic<sup>®</sup> F-127 Gel Formulations with Ketoconazole. *Int. J. Mol. Sci.* **2021**, *22*, 11326. [[CrossRef](#)] [[PubMed](#)]
42. Anwar, S.H.; Hasni, D.; Rohaya, S.; Antasari, M.; Winarti, C. The role of breadfruit OSA starch and surfactant in stabilizing high-oil-load emulsions using high-pressure homogenization and low-frequency ultrasonication. *Heliyon* **2020**, *6*, e04341. [[CrossRef](#)] [[PubMed](#)]
43. Lemaalem, M.; Ahfir, R.; Derouiche, A.; Filali, M. Static and dynamic properties of decane/water microemulsions stabilized by cetylpyridinium chloride cationic surfactant and octanol cosurfactant. *RSC Adv.* **2020**, *10*, 36155–36163. [[CrossRef](#)] [[PubMed](#)]
44. Jaiswal, P.; Aggarwal, G.; Harikumar, S.L.; Singh, K. Development of self-microemulsifying drug delivery system and solid-self-microemulsifying drug delivery system of telmisartan. *Int. J. Pharm. Investig.* **2014**, *4*, 195–206. [[CrossRef](#)] [[PubMed](#)]
45. Lukić, M.; Pantelić, I.; Savić, S.D. Towards optimal pH of the skin and topical formulations: From the current state of the art to tailored products. *Cosmetics* **2021**, *8*, 69. [[CrossRef](#)]
46. Hassan, D.S.; Hasary, H.J. The impact of viscosity on the dissolution of naproxen immediate-release tablets. *J. Taibah Univ. Med. Sci.* **2023**, *18*, 687–695. [[CrossRef](#)] [[PubMed](#)]
47. Djiobie Tchienou, G.E.; Tsatsop Tsague, R.K.; Mbam Pega, T.F.; Bama, V.; Bamseck, A.; Dongmo Sokeng, S.; Ngassoum, M.B. Multi-response optimization in the formulation of a topical cream from natural ingredients. *Cosmetics* **2018**, *5*, 7. [[CrossRef](#)]
48. Md, S.; Alhakamy, N.A.; Aldawsari, H.M.; Kotta, S.; Ahmad, J.; Akhter, S.; Shoab Alam, M.; Khan, M.A.; Awan, Z.; Sivakumar, P.M. Improved Analgesic and Anti-Inflammatory Effect of Diclofenac Sodium by Topical Nanoemulgel: Formulation Development—In Vitro and In Vivo Studies. *J. Chem.* **2020**, *2020*, 4071818. [[CrossRef](#)]
49. Fong Yen, W.; Basri, M.; Ahmad, M.; Ismail, M. Formulation and evaluation of galantamine gel as drug reservoir in transdermal patch delivery system. *Sci. World J.* **2015**, *2015*, 495271. [[CrossRef](#)]
50. Arora, R.; Aggarwal, G.; Harikumar, S.L.; Kaur, K. Nanoemulsion Based Hydrogel for Enhanced Transdermal Delivery of Ketoprofen. *Adv. Pharm.* **2014**, *2014*, 468456. [[CrossRef](#)]

51. Alhasso, B.; Ghori, M.U.; Conway, B.R. Development of Nanoemulsions for Topical Application of Mupirocin. *Pharmaceutics* **2023**, *15*, 378. [[CrossRef](#)] [[PubMed](#)]
52. Cox, S.D.; Mann, C.M.; Markham, J.L.; Gustafson, J.E.; Warmington, J.R.; Wyllie, S.G. Determining the antimicrobial actions of tea tree oil. *Molecules* **2001**, *6*, 87–91. [[CrossRef](#)]
53. Abreu, A.C.; Serra, S.C.; Borges, A.; Saavedra, M.J.; Mcbain, A.J.; Salgado, A.J.; Simoes, M. Combinatorial activity of flavonoids with antibiotics against drug-resistant *Staphylococcus aureus*. *Microb. Drug Resist.* **2015**, *21*, 600–609. [[CrossRef](#)] [[PubMed](#)]
54. Chaturvedi, P.; Singh, A.K.; Singh, A.K.; Shukla, S.; Agarwal, L. Prevalence of Mupirocin Resistant *Staphylococcus aureus* Isolates Among Patients Admitted to a Tertiary Care Hospital. *N. Am. J. Med. Sci.* **2014**, *6*, 403–407. [[CrossRef](#)]
55. Gangwar, A.; Kumar, P.; Singh, R.; Kush, P. Recent advances in mupirocin delivery strategies for the treatment of bacterial skin and soft tissue infection. *Future Pharmacol.* **2021**, *1*, 80–103. [[CrossRef](#)]

**Disclaimer/Publisher’s Note:** The statements, opinions and data contained in all publications are solely those of the individual author(s) and contributor(s) and not of MDPI and/or the editor(s). MDPI and/or the editor(s) disclaim responsibility for any injury to people or property resulting from any ideas, methods, instructions or products referred to in the content.